The Catalan Light Cone: A Recursive Substrate for Causal Geometry, Quantum Amplitudes, and Computation

Paul Fernandez

Abstract

We investigate the Catalan family of combinatorial structures—Dyck paths, full binary trees, and balanced parenthesis expressions—as a unified discrete substrate from which causal geometry, quantum amplitude propagation, and universal computation jointly emerge.

A central observation is that the Dyck constraint induces a natural causal order. When organized by growth tier and lateral spread, the Catalan lattice forms a discrete cone whose extremal configurations reproduce a light-cone–like causal envelope. Classical invariance-principle results show that constrained Dyck walks converge in the scaling limit to Brownian excursions. The associated continuum description is diffusive (governed by the heat operator on the half-line with the Dyck conditioning encoded by boundary conditions/conditioning), and under analytic continuation one recovers the free Schrödinger equation.

Via a uniform structural mapping—the pairs expansion—Dyck trees are placed in correspondence with SKI and λ-calculus term graphs, in the sense that Catalan tree shapes provide unlabeled application skeletons that can be equipped with standard finite encodings of symbols. Under this reading, causal extension aligns with functional application, while local collapse aligns with computational reduction. Structural equivalences of the substrate induce gauge-like redundancies, and disjoint subtrees commute analogously to spacelike-separated operators.

The paper distinguishes rigorously established correspondences—scaling limits, diffusion dynamics, prefix-causal structure, and computational universality in the sense of standard SKI/λ encodings—from conjectural extensions concerning measurement, actualization, and interaction structure.

Taken together, these correspondences show that a single recursive constraint can reproduce, at a structural and kinematical level, large portions of the operational framework of relativistic quantum theory and universal computation, without introducing additional primitives. We do not attempt to derive interactions or physical constants; the aim is to isolate the minimal recursive structure common to these domains.

1 Introduction

Discrete approaches to fundamental physics have long suggested that continuum spacetime and quantum dynamics may emerge from deeper combinatorial structure. Examples include causal sets [5], discrete random surfaces and Causal Dynamical Triangulations (CDT) [2, 3], spin networks and loop quantum gravity [16], tensor networks [15], and rewriting systems inspired by λ-calculus and combinatory logic.

Typically, however, these models require multiple independent ingredients: a relation or graph for causal structure, an algebra for computation, and additional rules for quantum propagation. This work explores a more economical possibility: that a *single* recursive structure simultaneously supports all three.

The focus is the *Catalan substrate*, the family of structures counted by the Catalan numbers [18], including Dyck paths, full binary trees, and balanced parenthesis expressions. These objects are usually studied in enumerative combinatorics, probability theory, and theoretical computer science. Here they are treated instead as a space of *admissible histories* generated by a minimal growth constraint. The central claim is that the Catalan substrate admits three tightly coupled interpretations:

(i) a discrete causal geometry with a light-cone–like envelope,

(ii) a natural path-integral dynamics with diffusive and wave-like continuum limits,

(iii) a universal computational calculus via λ- and SKI-term graphs.

These interpretations do not require distinct primitives; they arise from different readings of the same recursive object.

The geometric aspect follows from prefix order and growth bounds intrinsic to Dyck paths. The dynamical aspect follows from classical results on conditioned random walks and Brownian excursions [13, 11]. The computational aspect follows from the well-known equivalence between binary trees, cons-pair structures, and λ-calculus or SKI combinators [6, 9, 4]. Taken together, these results show that spacetime-like causal structure, quantum wave dynamics, and computation can be viewed as complementary manifestations of a single recursive substrate.

The exposition proceeds as follows. Section 2 establishes the discrete causal geometry of the Catalan lattice and its interpretation as a light cone. Subsequent sections place amplitude propagation and computation on this structure, analyze continuum limits, and discuss collapse, locality, and interaction. Optional coordinate embeddings, technical notes, and illustrative examples are collected in appendices, separate from the main formal development.

2 The Catalan Light Cone as a Discrete Causal Geometry

2.1 Dyck paths and growth tiers

A Dyck path of semilength n is a walk on the integers satisfying

$$H_{k+1} = H_k \pm 1, \qquad H_k \geq 0, \qquad H_0 = H_{2n} = 0.$$

Equivalently, Dyck paths are balanced parenthesis strings or full binary trees with n internal nodes. The number of such paths is the nth Catalan number

$$C_n = \frac{1}{n+1}\binom{2n}{n}.$$

Each up–down pair () represents a minimal unit of growth. The integer

$$t = n$$

will be called the *tier* and will be interpreted as a discrete proper time.

2.2 Prefix order and causality

Dyck paths carry a natural partial order by prefix inclusion. If a Dyck word u is a prefix of v, then u represents a causal ancestor of v. Conversely, prefixes that diverge represent causally incompatible futures. This prefix order defines a discrete causal structure:

- every node has a unique causal past,
- multiple incompatible futures may branch from the same prefix,
- cycles are prohibited by construction.

No additional causal axiom is required; causality is enforced combinatorially by the Dyck constraint.

2.3 Extremal configurations: chain and star

At fixed tier t there are many Dyck paths. Two extremal configurations play a distinguished role:

- the *chain* (or spine)
$$(((\cdots))),$$
fully nested, with maximal depth and minimal spread;
- the *star*
$$()()()\cdots(),$$
fully separated, with minimal depth and maximal spread.

All other configurations interpolate between these extremes. Together, the set of Dyck paths at tier t forms a discrete envelope bounded by the chain and the star.

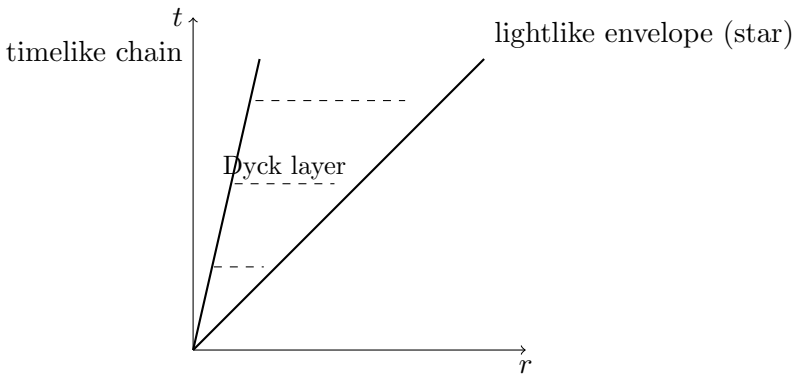

Figure 1: The Catalan light cone. Tier t (the number of Dyck units) plays the role of proper time, while breadth r measures spatial radius. All Dyck configurations at fixed tier lie between the fully nested chain (timelike extreme) and the fully separated star (lightlike envelope). Discrete Dyck layers approximate constant-time hypersurfaces, and the bound $r \le t$ is enforced combinatorially.

2.4 Breadth as spatial extent

Define the *breadth* $r(w)$ of a Dyck path w to be the size of a largest level set in the associated full binary tree:
$$r(w) := \max_{\ell}\{\text{number of nodes at depth } \ell\}.$$
Equivalently, $r(w)$ is the maximal number of non-overlapping pairs at a common nesting depth. For a Dyck word of tier t there are t matched pairs in total, so
$$1 \le r(w) \le t,$$

with $r = 1$ for the fully nested chain and $r = t$ for the fully separated star. The inequality

$$r \leq t$$

is enforced purely by the recursive constraint. It is the discrete analogue of the relativistic light-cone bound $|\Delta x| \leq \Delta t$ (in units with $c = 1$).

2.5 Depth–breadth tradeoff

Let $h(w)$ denote the maximum height of a Dyck path, i.e. the maximum nesting depth of its associated full binary tree (root at depth 0). Recall that the breadth $r(w)$ is the maximum number of nodes occurring at any fixed depth level:

$$r(w) := \max_{\ell} \text{number of nodes at depth } \ell.$$

Depth and breadth are not independent. In any full binary tree, the number of nodes at depth ℓ is at most 2^ℓ (each level can at most double from its parent level). Hence, if the maximum level set size $r(w)$ occurs at depth ℓ_*, then

$$r(w) \leq 2^{\ell_*} \leq 2^{h(w)} \quad \Rightarrow \quad h(w) \geq \log_2 r(w).$$

Thus configurations with large breadth necessarily have logarithmically large depth. Equivalently, very shallow trees cannot support wide level sets, while trees with very large depth must concentrate most nodes away from any single breadth-maximizing level.

Remark 2.1 (Kraft equality for leaf depths)**.** *For the full binary tree associated to a Dyck path, if L is the set of leaves and $d(\ell)$ denotes the depth of $\ell \in L$ (root at depth 0), then*

$$\sum_{\ell \in L} 2^{-d(\ell)} = 1.$$

Equivalently, the leaf depths form a complete binary prefix code. This gives a global constraint on allowable depth profiles beyond the crude level bound $r(w) \leq 2^{h(w)}$; see [7].

$((()))$	$(h = 3,\ r = 1)$
$(()())$	$(h = 2,\ r = 2)$
$(())()$	$(h = 2,\ r = 2)$
$()(())$	$(h = 2,\ r = 2)$
$()()()$	$(h = 1,\ r = 3)$

Figure 2: All Dyck words of tier $n = 3$, ordered from maximal nesting (chain) to maximal separation (star). These five configurations exhaust the discrete causal possibilities at fixed proper time. Depth h and breadth r interpolate between the two extremes, illustrating the intrinsic tradeoff enforced by the Dyck constraint. Higher tiers replicate this structure at larger scale.

2.6 Cone structure

Organizing Dyck paths by tier t and breadth r yields a discrete cone:

- each tier is a "constant-time" slice,
- the chain defines the timelike axis,
- the star defines the lightlike boundary,
- admissible configurations fill the interior.

This structure will be referred to as the *Catalan light cone*.

2.7 Scaling behavior

Classical results on conditioned random walks show that typical Dyck paths at tier t have height and breadth of order $\sqrt{t}$ [13, 11, 1]. Extremal configurations saturate the linear bound $r \leq t$, while typical configurations lie deep within the cone. This separation between extremal and typical behavior mirrors the role of null, timelike, and spacelike trajectories in relativistic geometry.

Theorem 2.1 (Discrete light-cone bound and scaling)**.** *Let w be a Dyck word of semilength t and breadth $r(w)$ as above. Then*

$$1 \leq r(w) \leq t.$$

Moreover, for a uniformly random Dyck word of semilength t, the typical height and breadth are of order $\sqrt{t}$.

The first statement follows from the definition of $r(w)$ and the fact that there are t internal nodes, while the scaling behavior is a consequence of invariance-principle results for conditioned random walks [13, 11, 1].

Coordinate charts and continuum comparisons. Appendix A collects optional coordinate-chart constructions (null-count embeddings and related continuum comparisons) used for intuition; the combinatorial results below do not depend on these embeddings.

2.8 Recursive Self-Similarity and Local Re-Centering

A key structural property of the Catalan substrate is its *recursive self-similarity*. Every Dyck word may be viewed as a node in the infinite prefix tree of admissible Dyck prefixes. At any such node u, with current height h and remaining length budget sufficient to return to height 0, the set of all admissible continuations of u forms a subtree whose shape is determined entirely by h. This subtree is canonically isomorphic to the Dyck-prefix tree that begins at height h rather than at height 0.

Formally, if $\mathcal{C}$ denotes the infinite Dyck-prefix tree and $\mathcal{C}_h$ denotes the Dyck-prefix tree conditioned to start at height h (i.e. with $H_0 = h$ and $H_k \geq 0$ for all k), then for every prefix u of height h we have a canonical isomorphism

$$\mathcal{C}(u) \;\cong\; \mathcal{C}_h.$$

Thus every node of the global Catalan possibility tree is the root of a scaled copy of the entire admissible-future structure, with scaling determined solely by local height. The recursive decomposition of full binary trees,

$$T = \bullet(T_L, T_R),$$

makes the same fact explicit in the tree representation: each subtree of a Catalan tree is itself a Catalan tree, and the decomposition applies inductively at every depth.

This recursive self-similarity has two important consequences for the geometric interpretation developed in this paper:

(i) **Locality and re-centering.** Because the admissible future of any prefix depends only on its present height, not on its global position, the Catalan light-cone geometry is *locally homogeneous*. The causal cone may be re-centered at any node without altering its shape: moving the focus does not change the structure of admissible futures, only the value of the local height at which the cone is rooted.

(ii) **Scale invariance of the substrate.** The same recursive rules govern growth at every depth. The local possibility space looks the same at all scales, in the sense that the subtree below any node is again Catalan. This is the combinatorial source of the invariance principles (Dyck $\to$ Brownian excursion) appearing in the continuum limit.

In summary, the Catalan substrate is self-similar at every node: each point in the possibility space contains a full Catalan future scaled by its current height. This allows the causal and geometric analysis of later sections to be performed relative to *any* node of the prefix tree. The light cone is not anchored to a global origin; it is an intrinsic, relocatable geometric feature of the recursive structure itself.

2.9 Multiple Local Cones and Relational Geometry

The recursive self-similarity of the Catalan substrate implies that there is not a single distinguished light cone rooted at the global origin. Instead, every node of the Dyck-prefix tree induces its own local notion of past, future, and lightlike boundary. This section records the combinatorial foundations of this phenomenon and its geometric consequences.

Cones rooted at arbitrary prefixes

Let u be any Dyck prefix with current height h. As shown in Section 2.8, the subtree $\mathcal{C}(u)$ of admissible continuations of u is canonically isomorphic to the Dyck-prefix tree $\mathcal{C}_h$ that begins at height h. Consequently, the structure of possible futures below u is itself a Catalan possibility space.

Define the *local cone at* u to be the set of all Dyck extensions of u, organized by length (tier) and breadth relative to u. The local chain is the fully nested extension of u, and the local star is the fully separated extension. These play the role of timelike and lightlike extremes for admissible growth below u.

Nested and divergent cones

Let u and v be Dyck prefixes.

(i) **Nested cones.** If u is a prefix of v, then $\mathcal{C}(v)$ is a subtree of $\mathcal{C}(u)$, and the local cone at v lies strictly inside the local cone at u. Their causal structures satisfy

$$\mathrm{Past}(v) \subset \mathrm{Past}(u), \qquad \mathrm{Future}(v) \subset \mathrm{Future}(u).$$

Thus cones nest hierarchically along any branch of the prefix tree.

(ii) **Divergent cones.** If neither prefix is contained in the other, then u and v share a common ancestor but diverge at some minimal prefix w. Their cones therefore have a shared causal past (the future of w up to u and v) but incompatible futures beyond that point. Formally,

$$\mathrm{Past}(u) \cap \mathrm{Past}(v) = \mathrm{Past}(w), \qquad \mathrm{Future}(u) \cap \mathrm{Future}(v) = \varnothing.$$

In this sense, divergent cones encode distinct branches of the Catalan possibility structure.

Relational geometry

These observations establish a relational geometric structure intrinsic to the Catalan substrate:

- every node induces its own local cone of admissible extensions;
- cones may be re-centered without changing their internal geometry;
- cones nest along causal chains and diverge after branching points;
- no global origin is privileged—only prefix order determines causal relationships.

This yields a family of interacting local cones, each encoding the admissible future relative to a chosen prefix. The Catalan light cone is therefore not a single global object but a *relocatable geometric feature* that appears at every node of the recursive substrate.

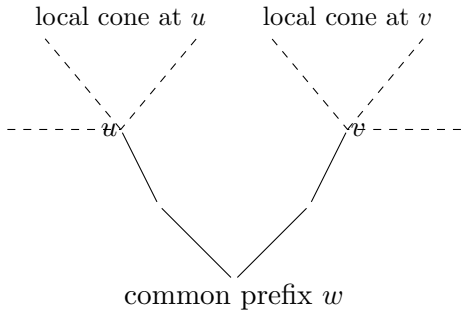

Figure 3: Two Dyck prefixes u and v diverging from a shared ancestor w. Dashed regions indicate the local Catalan cones rooted at u and v. Cones nest along causal chains and diverge after branching points, producing a family of local, relocatable causal geometries on the Catalan substrate.

2.10 Summary

The Catalan substrate supports a discrete causal geometry determined entirely by recursive constraint. Without introducing a manifold, metric, or causal relation by fiat, it yields:

- a partial order interpretable as causality,
- a cone-shaped causal envelope,
- intrinsic bounds on spatial extension,
- well-defined constant-time layers.

Subsequent sections place dynamical rules—quantum amplitudes and computational reduction—on this geometry.

3 Recursive Pairing and Universal Computation

3.1 Pairs expansion

Catalan Structure as the Space of Program Possibilities. The Catalan family—Dyck paths, full binary trees, and balanced-parenthesis expressions—forms the free magma on a single binary constructor. As observed in foundational work on the λ-calculus and combinatory logic [8, 4], every computable program has a canonical representation as a finite binary application tree: internal nodes encode application; leaves encode atomic symbols or combinators. Conversely, any finite binary tree equipped with leaf labels denotes a unique program modulo surface syntax. Thus the infinite Catalan tree is not merely a combinatorial object but the structural possibility space of all programs expressible in any Turing-complete functional calculus.

This observation also extends to operational semantics. Standard reductions (such as β-reduction or SKI contraction) are local rewrite rules on binary trees, and the pairs-expansions of combinators remain within the Catalan family. Accordingly, a program, its intermediate expansion frames, and each permissible reduction schedule are all representable as paths through a single Catalan substrate. Selecting a program shape or selecting a specific reduction history is therefore equivalent to selecting a path in the Catalan tree. In this sense the Catalan substrate uniformly encodes program syntax, program semantics, and the full ensemble of admissible computational histories.

Proposition 3.1 (Catalan Universality for Program Structure)**.** *Let $\mathcal{C}$ denote the Catalan family of finite full binary trees. Every program in any Turing-complete functional calculus (such as the λ-calculus or SKI) admits a canonical representation as an element of $\mathcal{C}$ with leaf labels drawn from a finite alphabet. Conversely, every labeled element of $\mathcal{C}$ denotes a unique program modulo surface syntax. Furthermore, standard operational semantics (including β-reduction and SKI contraction) act as local rewrite rules that preserve membership in $\mathcal{C}$. Thus a program, its syntactic expansions, and every admissible reduction history correspond to paths within the Catalan substrate.*

A proof sketch and illustrative examples are provided in Appendix D.

Two canonical parenthesis encodings. There are (at least) two particularly useful parenthesis-only encodings of a full binary tree:

- **Dyck encoding** ("walk" view): balanced parentheses of length $2t$, naturally adapted to height profiles and scaling limits.
- **Pairs (S-expression) encoding** ("cons" view): write each leaf as `()` and each internal node as a parenthesized pair of its two children, i.e. $T = (L, R) \mapsto (\texttt{enc}(L)\,\texttt{enc}(R))$. This is a variable- and label-free Lisp-style representation with `()` as the only atom.

In particular, in the *pairs* encoding, the smallest object is the empty pair `()`, and the smallest nontrivial *binary* object is `(()())`, i.e. a root pair whose two children are leaves. In the Dyck encoding, the semilength-1 object is `()`, since Dyck words begin only after the first matched pair exists.

3.2 A small tier shown three ways (Dyck / tree / pairs)

Figure 4 augments the standard Dyck-$n = 3$ list by displaying, for the *same* five Catalan shapes, the corresponding pairs (S-expression) encodings.

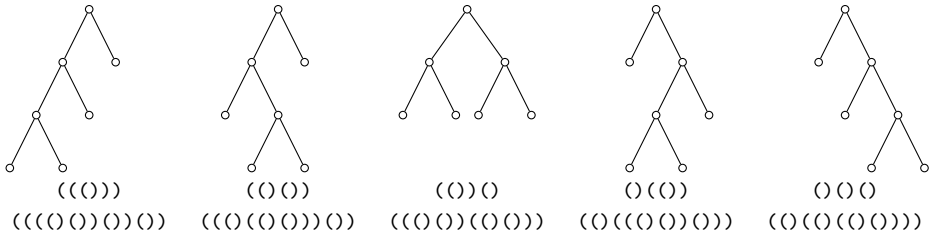

Figure 4: The five Catalan shapes at tier $t = 3$ shown as (i) Dyck words, (ii) full binary trees, and (iii) pairs (S-expression) encodings in which each leaf is `()` and each internal node is a parenthesized pair of its two children (as if one were looking "down into" the tree). These are three coordinate systems for the same underlying Catalan objects.

3.3 Connection to λ-calculus and SKI

Binary trees are a standard representation of λ-terms and SKI combinators [6, 9, 4]. Variables may be represented by leaf positions, abstraction by structural capture, and application by tree composition. Under the pairs expansion, each Dyck tree canonically determines an unlabeled application graph. When variables are suppressed, the resulting graphs coincide with the structure graphs used in combinatory logic. No additional primitives beyond recursive pairing are required to obtain this representation.

Choosing a finite set of tree patterns to represent the SKI combinators and interpreting local tree rewrites as SKI reduction therefore equips the Catalan substrate with a standard universal calculus: every partial recursive function can be encoded as an SKI term, and hence by a finite Dyck tree, and every computation corresponds to a sequence of local tree transformations. In this sense, the Catalan substrate is *computationally universal*. What is new here is that the same underlying objects simultaneously carry a causal and geometric interpretation.

3.4 Reduction and local collapse

In the computational interpretation, reduction corresponds to local pattern replacement. A redex occupies a finite region of a tree and may be reduced without reference to distant subtrees. This locality mirrors the causal structure established in Section 2. From the perspective of the Catalan lattice, reduction may be viewed as *collapse*: a locally ambiguous structure is replaced by a simpler one consistent with the global constraint. Importantly, collapse does not alter causal ancestry; it refines an already-admissible history. For standard calculi (e.g. λ/SKI), confluence ensures uniqueness of normal forms when they exist, and more locally reductions supported on disjoint subtrees commute. This computational fact will later support an interpretation of spacelike commutativity.

3.5 Summary

Recursive pairing suffices to encode universal computation. Via the pairs expansion, Dyck trees and application graphs are two views of the same structure. Local computational reduction aligns naturally with causal locality on the Catalan light cone.

4 Quantum Amplitudes on the Catalan Lattice

4.1 Histories as paths

Interpreting Dyck paths as admissible histories motivates assigning weights to each history. Let $\mathcal{D}_t$ denote the set of Dyck paths of tier t. A state at tier t may be represented as a formal superposition of histories

$$\Psi_t = \sum_{w \in \mathcal{D}_t} \psi(w) \, |w\rangle.$$

Local extensions of a Dyck path correspond to admissible future steps. Thus, time evolution is governed by transitions that respect the Dyck constraint.

4.2 Observables, projection, and coherent summation

Fix a tier t and consider the set $\mathcal{D}_t$ of Dyck paths of semilength t. Each $w \in \mathcal{D}_t$ represents a complete admissible history at discrete time t, with an associated height profile

$$H_w : \{0, 1, \ldots, 2t\} \to \mathbb{Z}_{\geq 0}.$$

An observable is defined as a deterministic coarse-graining

$$f : \mathcal{D}_t \to \mathcal{X},$$

where $\mathcal{X}$ is a discrete set of outcomes corresponding to a chosen equivalence relation on histories. An outcome $x \in \mathcal{X}$ corresponds to the equivalence class $f^{-1}(x) \subset \mathcal{D}_t$ of histories. By construction, such a projection discards information: many distinct histories may be identified as the same observable outcome.

With no additional structure imposed, the natural measure on $\mathcal{D}_t$ is uniform counting. The induced distribution on the outcome space $\mathcal{X}$ is therefore the pushforward of the uniform counting measure,

$$N(x) := \#\{w \in \mathcal{D}_t : f(w) = x\}.$$

Even with uniform weight on histories, the induced distribution on $\mathcal{X}$ is generically non-uniform, reflecting the combinatorial geometry of the projection rather than any imposed dynamics.

A discrete analogue of an integral along a history is given by the step-sum of the height profile,

$$A(w) := \sum_{k=0}^{2t-1} H_w(k),$$

which measures the cumulative dwell time at nonzero height. This quantity depends on the full distribution of height along the path, not merely on extrema such as maximum height or peak count.

From this additive structural functional one may define a complex phase

$$\theta(w) := \alpha \, A(w), \qquad \psi(w) := e^{i\theta(w)},$$

where α is a global scale parameter. No per-path phase assignment is introduced; distinct phases arise solely from differences in the distribution of height over the history.

Given an observable f, the complex amplitude associated with an outcome $x \in \mathcal{X}$ is the coherent sum

$$\Psi(x) := \sum_{w:\, f(w)=x} \psi(w),$$

and observed probabilities are obtained by normalization of squared magnitudes,

$$P(x) = \frac{|\Psi(x)|^2}{\sum_{x' \in \mathcal{X}} |\Psi(x')|^2}.$$

Thus histories that are indistinguishable under the observable f are combined prior to squaring, while distinguishable histories are not. Interference is therefore a generic consequence of assigning complex weights to histories and summing coherently over coarse-grained equivalence classes before applying the Born rule.

Optional: coarse-graining entropy. Appendix B records an optional entropy bookkeeping for coarse-grainings and collapse counts.

4.3 Path integrals and conditioned walks

Dyck paths are random walks conditioned to remain nonnegative and return to zero. Classical results show that, when rescaled appropriately, ensembles of such paths converge to Brownian excursions [13, 11]. Assigning equal weight to all admissible paths yields a discrete path integral. More general amplitude assignments may depend on local features such as height or curvature, provided the Dyck constraint is preserved.

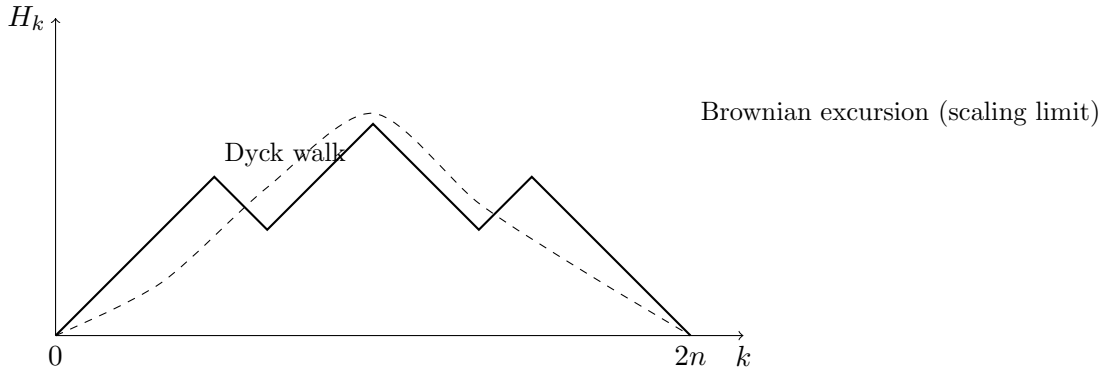

Figure 5: A Dyck path as a nearest-neighbour walk (H_k) constrained to stay nonnegative and return to zero at time $2n$. Under diffusive rescaling of k and H_k, ensembles of such paths converge to Brownian excursions, providing the bridge to the heat and Schrödinger equations discussed in the text.

Optional stratifications. Appendix B discusses Narayana stratification by peak count as an optional organizing tool.

4.4 Discrete path-integral formulation

The preceding constructions admit a direct interpretation as a discrete path integral on the Catalan light cone. Fix a tier t and an observable $f : \mathcal{D}_t \to \mathcal{X}$, where $\mathcal{X}$ is a finite set of outcomes

corresponding to a chosen coarse-graining of histories. Each Dyck path $w \in \mathcal{D}_t$ represents a complete admissible history, and the projection f determines which distinctions between histories are retained and which are discarded.

Define a complex weight for each history by

$$\psi(w) = e^{i\alpha A(w)},$$

where

$$A(w) = \sum_{k=0}^{2t-1} H_w(k)$$

is the discrete height integral introduced above. The amplitude associated with an observable outcome $x \in \mathcal{X}$ is then

$$\Psi(x) = \sum_{w:\, f(w)=x} e^{i\alpha A(w)}.$$

This expression is formally identical to a path integral: the amplitude is a sum over all admissible histories compatible with the observable outcome, with each history contributing a phase determined by an additive functional. No continuum limit, action functional, or variational principle is assumed at this stage; the structure arises purely from discrete combinatorics.

Several features commonly associated with continuum path integrals are already present:

(i) **Sum over histories.** All admissible Dyck paths consistent with the observable contribute. The Dyck constraint enforces causal admissibility in the same way that restrictions on allowed paths do in relativistic path integrals.

(ii) **Additive phase functional.**

The quantity $A(w)$ is additive under concatenation of path segments and depends only on the local height increments. It therefore plays the role of a discrete action accumulated along the history.

(iii) **Interference from coarse-graining.** Interference arises precisely because the observable f fails to distinguish between certain histories. Histories that are identified by the projection are summed coherently, while those distinguished by the observable are not.

(iv) **Gauge redundancy.** Different Dyck paths may correspond to the same abstract computation or the same coarse-grained structure, differing only by the ordering of spacelike-separated updates. The path integral sums coherently over such gauge-equivalent histories, while observable probabilities depend only on the resulting amplitudes.

From this perspective, the Catalan lattice provides a discrete realization of the sum-over-histories principle in which both the space of histories and the phase functional are combinatorially well defined. In the next subsection we show that, under appropriate scaling limits, this discrete formulation converges to familiar continuum descriptions governed by diffusion and Schrödinger dynamics.

Concrete physical measurements may be modeled by choosing observables that retain geometric features of a history (such as transverse displacement at a fixed tier). No such spatial interpretation, however, is required for the formal development.

For readers seeking a concrete intuition for how this discrete sum-over-histories mechanism produces interference, Appendix C sketches a finite thought experiment analogous to the double-slit experiment.

4.5 Scaling of the area phase in the continuum limit

The interference mechanism above assigns each history $w \in \mathcal{D}_n$ a complex weight $\psi(w) = e^{i\alpha A(w)}$ with discrete area functional

$$A(w) := \sum_{k=0}^{2n-1} H_w(k),$$

where $H_w(k)$ is the height after k steps.

To relate this discrete phase to the diffusion scaling limit, introduce the rescaled height process on $[0, 1]$,

$$X^{(n)}(\tau) := n^{-1/2} H_w(\lfloor 2n\tau \rfloor), \qquad 0 \le \tau \le 1.$$

Under the standard Dyck-to-Brownian-excursion scaling, $X^{(n)} \Rightarrow X$ in distribution, where X is a Brownian excursion on $[0, 1]$.

The discrete area rescales as a Riemann sum:

$$\frac{1}{2n^{3/2}} A(w) = \frac{1}{2n} \sum_{k=0}^{2n-1} n^{-1/2} H_w(k) \implies \int_0^1 X(\tau)\, d\tau.$$

Consequently, a nontrivial continuum phase is obtained by scaling α with n as

$$\alpha_n := \frac{\lambda}{2n^{3/2}},$$

so that

$$e^{i\alpha_n A(w)} \implies \exp\Big(i\lambda \int_0^1 X(\tau)\, d\tau\Big).$$

This makes explicit that the discrete coherent sum with additive functional $A(w)$ converges to a continuum functional weight. In particular, when one passes from uniform counting of conditioned walks to diffusion limits, inserting the exponential of a time-integrated functional corresponds (at the PDE level) to adding a potential term (via the standard Feynman–Kac mechanism). Setting $\lambda = 0$ recovers the unweighted scaling limit discussed in the next subsection.

4.6 Diffusion limit

Let $n \to \infty$ and rescale time and height by

$$t \mapsto n\tau, \qquad h \mapsto \sqrt{n}\, x.$$

Under this scaling, the probability density $\rho(\tau, x)$ for conditioned walks converges in law to that of a Brownian excursion on $x \ge 0$. At the PDE level, the associated continuum evolution is governed by the heat operator on the half-line, with the Dyck conditioning encoded by appropriate boundary/conditioning at $x = 0$. In particular, one obtains a heat equation of the form

$$\partial_\tau \rho = \frac{1}{2}\, \partial_x^2 \rho, \tag{1}$$

with the boundary/conditioning determined by the chosen scaling limit and conditioning. Full derivations may be found in [13, 11].

4.7 Schrödinger equation

More formally, if $\rho(\tau, x)$ denotes the real heat kernel on $x \geq 0$, analytic continuation in the diffusion parameter, $\tau \mapsto it$, produces a complex-valued kernel $\psi(t, x)$ satisfying the free Schrödinger equation

$$i\partial_t \psi = -\frac{1}{2}\,\partial_x^2 \psi. \tag{2}$$

Boundary conditions at $x = 0$ are carried over from the diffusive regime (e.g. reflecting or absorbing), and the choice of boundary does not affect the existence of the continuum limit itself. Thus, quantum wave dynamics arises here as the analytic continuation of diffusive propagation on the Catalan lattice, in line with the classical connection between diffusion and Schrödinger evolution [10, 12]. No separate quantization procedure is required; the wave equation is inherited from the scaling limit of constrained combinatorial growth.

5 Locality, Commutation, and Interaction

5.1 Disjoint subtrees

Two subtrees of a Dyck tree that share no common ancestor beyond a given prefix are causally independent. Operations localized to one subtree do not affect the other. In the computational interpretation, this corresponds to independent reductions. In the amplitude interpretation, it corresponds to commuting operators acting on spacelike-separated regions. Multiple Dyck paths may represent the same abstract computation or the same coarse-grained geometry. Such redundancies may be quotiented out without changing observable predictions, yielding equivalence classes of histories. This redundancy plays a role analogous to gauge symmetry: distinct internal descriptions correspond to the same external behavior.

Operationally, gauge here means a redundancy in the description of histories. For a fixed initial tree, consider the class of causal histories that apply the same multiset of local reductions but differ only in the temporal ordering of reductions supported on disjoint subtrees. Such histories are gauge-equivalent: they represent the same physical pattern of events, and their linear orderings are related by commuting spacelike-separated updates. The resulting equivalence classes (gauge orbits) play the role of physical histories, while genuinely different choices of which reductions to actualize belong to distinct orbits and define the nontrivial branching structure of the multiway reduction graph.

(See Appendix D, and in particular Lemma D.1, for a formal statement and proof sketch of the corresponding disjoint-commutation property.)

5.2 Collapse and selection

Both computation and amplitude propagation require selection:

- computational reduction chooses a redex,
- measurement-like selection chooses an observable outcome, corresponding to an equivalence class under the chosen projection.

In the Catalan substrate, selection operates locally, refining rather than destroying structure. The global constraint ensures consistency after selection. The formal development of collapse probabilities lies beyond the scope of this paper and is treated here only structurally.

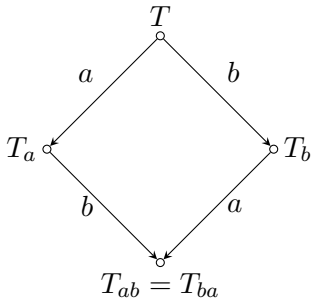

Figure 6: Local diamond for commuting disjoint updates. Starting from a common state T, two spacelike-separated reductions a and b can be applied in either order, yielding intermediate states T_a and T_b but the same final state $T_{ab} = T_{ba}$. The two intermediate events are spacelike-separated: they share a common past (T) and a common future (T_{ab}) but no causal edge between them. This expresses microcausality on the Catalan substrate: local updates supported on disjoint subtrees commute and differ only by a gauge choice of temporal ordering.

5.3 Summary

Locality, commutation, and interaction emerge directly from the causal and recursive structure of the Catalan lattice. The same principles underlie both computational reduction and quantum amplitude propagation.

6 Discussion and Limitations

The results presented here establish a shared structural basis for causal geometry, quantum dynamics, and computation. Several limitations should be emphasized:

- Physical constants and interactions are not derived.
- Only free (noninteracting) wave dynamics appears explicitly.
- Collapse probabilities are not fixed uniquely by the structure.

These limitations reflect a deliberate restriction of scope. The goal has been to isolate the minimal recursive structure common to multiple domains, not to provide a complete physical theory.

6.1 Relation to discrete quantum gravity

Similar scaling behavior appears in two-dimensional quantum gravity and random surface models. In particular, Causal Dynamical Triangulations (CDT) enforce a preferred foliation and causal constraint that parallels the prefix order of Dyck paths [2, 3]. In CDT, the continuum limit is taken after summing over causally admissible triangulations. Here the admissible structures are Dyck paths rather than triangulations, but the organizing principle—the restriction to histories that respect a causal growth rule—is closely analogous.

7 Conclusion

This paper has examined the Catalan family of recursive structures as a common substrate for causal geometry, quantum amplitude propagation, and computation. The Dyck constraint induces

a natural causal order and a discrete cone-shaped geometry exhibiting light-cone–like bounds. Classical invariance principles show that ensembles of admissible histories converge in the continuum limit to Brownian excursions, leading to diffusive continuum limits governed by the heat operator (with the Dyck conditioning encoded on the half-line) and, under analytic continuation, the free Schrödinger equation. Through the pairs expansion, the same structures encode universal computation via λ-calculus and SKI combinators. These correspondences require no additional primitives beyond recursive pairing and constraint. Spacetime-like geometry, wave dynamics, and computation emerge as complementary aspects of a single recursive system. Several open problems remain, including the incorporation of interaction terms, the determination of collapse probabilities, and the connection to physical constants. The results presented here establish a minimal and structurally unified foundation upon which such extensions may be explored.

A Coordinate Charts and Continuum Comparisons

This appendix collects optional coordinate embeddings and continuum comparisons used for intuition; the combinatorial results in the main text do not depend on these constructions.

A.1 Coordinate charts on the Catalan cone

Remark A.1 (Notation hygiene)**.** *To avoid collisions, the* tier *(semilength) of a completed history is denoted by n. A* prefix length *is denoted by $k \in \{0, 1, \ldots, 2n\}$. Within this subsection only, the symbols (t_k, x_k) denote an* embedded *spacetime chart derived from cumulative counts (Definition A.1), and should not be confused with the tier index n used elsewhere.*

The Catalan cone as the master object. Let $\mathcal{C}$ denote the set of Dyck prefixes (balanced-parentheses *prefixes* that never go below height 0), partially ordered by extension: $p \preceq q$ iff q has prefix p. A completed history is a maximal element $w \in \mathcal{D}_n \subset \mathcal{C}$ of semilength n. For any prefix $p \in \mathcal{C}$, the future

$$\mathcal{C}(p) \;:=\; \{\, q \in \mathcal{C} : p \preceq q \,\}$$

is canonically a "local cone" rooted at p: the same growth law, re-centered. Thus there is a single substrate $\mathcal{C}$ (and its re-rootings), and different "cones" arise from different coordinate charts or coarse-grainings of this same object.

Two cumulative counts and a light-cone chart. The most rigid chart on $\mathcal{C}$ is obtained by tracking the cumulative numbers of opens and closes.

Definition A.1 (Null counts and embedded coordinates)**.** *Fix a Dyck word $w \in \mathcal{D}_n$, and let $w[1{:}k]$ denote its length-k prefix. Define*

$$u(k) \;:=\; \#\{\text{(in } w[1{:}k]\},\qquad v(k) \;:=\; \#\{\text{) in } w[1{:}k]\}.$$

The Dyck admissibility constraint is $u(k) \geq v(k)$ for all k, and completion is $u(2n) = v(2n) = n$. Define the height (frontier) process

$$H(k) \;:=\; u(k) - v(k) \;\geq\; 0,$$

and the embedded "spacetime" coordinates

$$t_k \;:=\; \frac{u(k) + v(k)}{2} \;=\; \frac{k}{2},\qquad x_k \;:=\; \frac{u(k) - v(k)}{2} \;=\; \frac{H(k)}{2}.$$

Equivalently $u = t_k + x_k$ and $v = t_k - x_k$ (a discrete null-coordinate form).

Under this embedding, each symbol advances time and changes space by one unit (up to the 1/2 normalization):

$$\texttt{(}:\ (t,x)\mapsto(t+\tfrac{1}{2},\ x+\tfrac{1}{2}),\qquad \texttt{)}:\ (t,x)\mapsto(t+\tfrac{1}{2},\ x-\tfrac{1}{2}).$$

Hence the path stays inside the cone $|x_k| \le t_k$, with the boundary $x_k = 0$ representing zero frontier (no outstanding opens).

Why "return to 0" is not "return to the origin." The completion constraint $H(2n) = 0$ means only that the *imbalance* vanishes: every open has been matched by a close. In spacetime coordinates, the endpoint is

$$(t_{2n}, x_{2n}) \ = \ \big(n, 0\big),$$

not $(0, 0)$. Thus a history expands monotonically in t (prefix length grows), while the spatial coordinate x is a *frontier variable* that eventually returns to 0 because no unfinished structure may remain at completion.

Pairs, trees, and S-expressions are identical structure. A Dyck word w can be read as a parenthesized S-expression skeleton, and it already *is* a rooted ordered tree: matched parenthesis pairs are nodes; containment defines parent/child; and left-to-right order in the string gives sibling order. For example, $w = \texttt{(()())}$ has one outer pair (the root) containing two inner pairs (two leaves). Under this identification, the height $H(k)$ is the number of currently-open pairs—the size of the *active frontier* of the tree under construction.

Evaluation "return" as frontier discharge. If evaluation is recorded at the level of control (continuations), then entering a subproblem pushes a context frame and finishing it pops that frame. In a well-bracketed evaluation regime, this push/pop trace is Dyck, and the same counts $(u(k), v(k))$ track control events. The embedded coordinate x_k therefore measures continuation depth (pending contexts), and the return to $x = 0$ at termination is the emptying of the continuation stack: no pending contexts remain. Value return is mediated by this control return; the Dyck "return" is fundamentally the discharge of outstanding obligations.

Breadth as a different projection (history-level, not frontier-level). Statistics such as breadth $r(w)$ summarize a *completed* history by the maximum size of a constant-depth slice in its associated tree. This is a coarse-graining of w (many distinct histories share the same (n, r)), and it should be distinguished from the frontier coordinate x_k, which is an instantaneous depth/obligation variable along a single prefix trajectory.

Summary of the two readings. There is one substrate $\mathcal{C}$ (and its re-rooted futures $\mathcal{C}(p)$). Two useful "cone" pictures arise from: (i) the embedded prefix trajectory (t_k, x_k) derived from null counts (pathwise frontier dynamics), and (ii) history-level projections such as $(n, r(w))$ (coarse geometric envelope). The pairs/tree/S-expression view does not introduce a new object; it is an identity of representations of the same Catalan structure.

A.2 Dyck Coordinates, Lorentz Geometry, and Computational Proper Time

Remark A.2 (Indices and coordinate conventions)**.** *Throughout, n denotes the tier (semilength) of a completed Dyck history. Within this subsection, $k \in \{0, 1, \ldots, 2n\}$ denotes a* step index *along*

a single history, and m denotes the number of collapse events *(local redex contractions) performed by a chosen evaluation strategy.*

A Dyck history $w \in \mathcal{D}_n$ induces an integer-valued nearest-neighbour walk $(H_k)_{k=0}^{2n}$ (the height / nesting depth signal) with

$$H_{k+1} = H_k \pm 1, \qquad H_0 = 0, \qquad H_k \geq 0, \qquad H_{2n} = 0.$$

Define the rescaled coordinates

$$t_k := \frac{k}{2}, \qquad x_k := \frac{H_k}{2},$$

so that each parenthesis advances time by $\frac{1}{2}$ and changes the transverse coordinate by $\pm\frac{1}{2}$:

$$(: \ (t,x) \mapsto (t+\tfrac{1}{2},\ x+\tfrac{1}{2}), \qquad): \ (t,x) \mapsto (t+\tfrac{1}{2},\ x-\tfrac{1}{2}).$$

For any walk with steps $(\Delta t, \Delta x) = (\frac{1}{2}, \pm\frac{1}{2})$ one has the kinematic cone bound $|x_k - x_0| \leq t_k - t_0$. In the Dyck case, the additional constraint is one-sided: $x_k \geq 0$ for all k, together with the endpoint condition $x_{2n} = 0$. Thus Dyck histories occupy the right half of a discrete light cone and return to the axis only at completion.

Introduce discrete null coordinates (compare Definition A.1)

$$u := t + x, \qquad v := t - x.$$

In continuum $(1+1)$-dimensional Minkowski space, a Lorentz boost with rapidity η acts linearly as

$$u' = e^{\eta} u, \qquad v' = e^{-\eta} v, \tag{3}$$

and transforming back to (t, x) yields the standard Lorentz transformation

$$t' = \gamma(t - v_L x), \qquad x' = \gamma(x - v_L t), \tag{4}$$

where

$$\gamma = \frac{1}{\sqrt{1 - v_L^2}}, \qquad v_L = \tanh \eta,$$

in units $c = 1$. The Minkowski interval

$$\mathrm{d}s^2 = \mathrm{d}t^2 - \mathrm{d}x^2 \tag{5}$$

is invariant under (4). In this sense the step rule supplies a discrete null-step kinematics, while the Dyck constraint supplies the boundary and return conditions selecting the Catalan ensemble. We emphasize that generic nontrivial boosts do not preserve the discrete Dyck lattice itself (the counts u, v are integers), so the Lorentz discussion here is a continuum comparison for the embedded coordinates rather than a discrete symmetry claim.

Computational proper time. A reduction history carries an intrinsic progress parameter given by the count of collapse events. Let m be the number of local redex contractions performed by an evaluation strategy up to a given stage, and define the *computational proper time*

$$\tau := \alpha\, m, \tag{6}$$

where $\alpha > 0$ is the characteristic scale associated with a single collapse. In continuum Minkowski space, a parametrized world-line $(t(s), x(s))$ admits a proper-time functional

$$\left(\frac{\mathrm{d}\tau}{\mathrm{d}s}\right)^2 = \left(\frac{\mathrm{d}t}{\mathrm{d}s}\right)^2 - \left(\frac{\mathrm{d}x}{\mathrm{d}s}\right)^2, \tag{7}$$

which is Lorentz-invariant under (4). In the present discrete setting, Equation (6) is simply a well-defined event-count parameter; the analogy is that collapse count plays the role of a proper-time progress variable along a chosen computational history.

B Additional Technical Notes

B.1 Entropy of coarse-graining and information rate

Fix a tier t and an observable (deterministic coarse-graining) $f : \mathcal{D}_t \to \mathcal{X}$. For $x \in \mathcal{X}$ write

$$N(x) \;:=\; \#\{w \in \mathcal{D}_t : f(w) = x\},$$

so that $f^{-1}(x)$ is the equivalence class of histories identified as the same outcome.

Multiplicity entropy. Define the (microcanonical) entropy of the full ensemble at tier t by

$$S_t \;:=\; \log \#(\mathcal{D}_t),$$

and the conditional entropy of an outcome x by

$$S(x) \;:=\; \log N(x).$$

The information eliminated by selecting outcome x is the entropy drop

$$\Delta S(x) \;:=\; S_t - S(x) \;=\; \log\Big(\frac{\#(\mathcal{D}_t)}{N(x)}\Big).$$

(Any logarithm base may be used; base 2 yields units of bits.)

Information rate as rate of possibility reduction. Let k denote the number of selection events (local contractions) along a history, and let computational proper time be $\tau = \tau_0 k$ for a fixed scale $\tau_0 > 0$. We define the information rate associated with outcome x to be the information loss per unit computational proper time,

$$R(x) \;:=\; \frac{\Delta S(x)}{\tau}.$$

In the simplest case of a single event ($k = 1$), this reduces to $R(x) = \Delta S(x)/\tau_0$.

Proposition B.1 (Basic properties)**.** *For any observable $f : \mathcal{D}_t \to \mathcal{X}$:*

(i) (Nonnegativity) $\Delta S(x) \geq 0$ for all attainable $x \in \mathcal{X}$, with equality iff $N(x) = \#(\mathcal{D}_t)$ (i.e. f is constant on $\mathcal{D}_t$).

(ii) (Additivity under independent factorization) If $\mathcal{D}_t$ factorizes as a Cartesian product $\mathcal{D}_t \cong \mathcal{D}_t^{(1)} \times \mathcal{D}_t^{(2)}$ and $f(w_1, w_2) = (f_1(w_1), f_2(w_2))$, then

$$\Delta S(x_1, x_2) = \Delta S_1(x_1) + \Delta S_2(x_2).$$

Proof. (i) Since $1 \leq N(x) \leq \#(\mathcal{D}_t)$ whenever x is attainable, the ratio $\#(\mathcal{D}_t)/N(x) \geq 1$, hence $\Delta S(x) \geq 0$, with equality exactly when $N(x) = \#(\mathcal{D}_t)$. (ii) Under the stated factorization, $N(x_1, x_2) = N_1(x_1)N_2(x_2)$ and $\#(\mathcal{D}_t) = \#(\mathcal{D}_t^{(1)})\#(\mathcal{D}_t^{(2)})$, so ΔS splits as a sum. □

Gauge-invariant counting. When histories admit a redundancy under commuting spacelike-separated updates, one may quotient $\mathcal{D}_t$ by the induced gauge equivalence relation $\sim_g$ and define $\bar{\mathcal{D}}_t := \mathcal{D}_t/\sim_g$. If f is gauge-invariant (constant on $\sim_g$-orbits), define

$$\bar{N}(x) := \#\{[w] \in \bar{\mathcal{D}}_t : f(w) = x\}, \qquad \bar{\Delta S}(x) := \log\Big(\frac{\#(\bar{\mathcal{D}}_t)}{\bar{N}(x)}\Big),$$

and use $\bar{\Delta S}$ in place of ΔS. This removes overcounting due solely to reordering of independent collapses.

B.2 Narayana stratification and structural modes

Dyck paths admit a natural finite stratification by peak count. For $w \in \mathcal{D}_t$, define its *peak count* $K(w)$ as the number of indices $k \in \{1, \dots, 2t-1\}$ at which the Dyck word has an up-step immediately followed by a down-step (equivalently, the number of local maxima of the height profile $H_w(k)$). The Narayana numbers $N(t,k)$ count the number of Dyck paths with $K(w) = k$, yielding the partition

$$\mathcal{D}_t = \bigsqcup_{k=1}^{t} \mathcal{D}_{t,k}, \qquad \mathcal{D}_{t,k} := \{w \in \mathcal{D}_t : K(w) = k\}.$$

To make the notion of "mode" precise, embed each history into a finite inner-product space. Let

$$V_t := \mathbb{R}^{2t+1}, \qquad H(w) := (H_w(0), \dots, H_w(2t)) \in V_t,$$

with standard inner product

$$\langle a, b\rangle := \sum_{j=0}^{2t} a_j b_j.$$

Fix an orthonormal basis $\{\phi_m\}_{m=0}^{2t}$ of V_t (for example, the discrete cosine basis or the eigenvectors of the discrete Laplacian on the path graph). The coefficients

$$c_m(w) := \langle H(w), \phi_m\rangle$$

define a spectral decomposition of the history w, with power spectrum $P_m(w) := |c_m(w)|^2$.

The peak count $K(w)$ does not label a single spectral mode. Rather, it provides a coarse combinatorial proxy for oscillatory complexity of the height signal. A natural summary statistic for how a Narayana class distributes spectral weight is the conditional mean spectrum

$$\overline{P}_m(t,k) := \mathbb{E}[\, P_m(w) \mid w \in \mathcal{D}_{t,k}]\,.$$

Intuitively, larger k tends to shift weight toward higher spectral indices m, reflecting more frequent alternation of slopes; this heuristic may be used as a discrete analogue of increased high-frequency content.

Finally, since the phase functional used in Section 4 depends on the full height profile (e.g. $\theta(w) = \alpha A(w)$), differences in peak placement within a fixed Narayana class generally change $A(w)$ and hence the phases appearing in coherent summation. Interference therefore depends both on coarse stratification by $K(w)$ and on finer structural variation within each class.

C A Double-Slit Thought Experiment on the Catalan Light Cone

This appendix provides an illustrative thought experiment showing how the discrete path-integral formalism developed in Section 4 exhibits interference in a setting analogous to the double-slit experiment. The construction is entirely combinatorial and finite. No new assumptions, dynamical rules, or continuum limits are introduced; the purpose is solely to instantiate the formalism in a familiar narrative.

C.1 Two sources as boundary-conditioned cones

Consider two distinct Dyck prefixes u_L and u_R of equal length and height. Each prefix induces a local Catalan cone of admissible continuations, as described in Section 2.9. We refer to these as the left and right source cones, although no spatial interpretation is assumed at this stage.

Both cones are evolved to a common tier n, producing two ensembles of Dyck paths of semilength n that differ only in their initial boundary condition. The admissible histories from both cones are evaluated relative to the same observable defined below.

C.2 Observable and indistinguishability

Fix a tier n and define an observable

$$f : \mathcal{D}_n \to \mathcal{X},$$

where $\mathcal{X}$ is a discrete outcome space. The observable f retains a coarse-grained feature of each history (for example, a bin determined by the mean height or total area) and discards all other information, including which source cone the history originated from.

Interference arises precisely because histories originating from distinct cones may be rendered indistinguishable by the observable. If the observable were to retain source information, no interference would occur.

C.3 Enumeration of histories at $n = 3$

At semilength $n = 3$, the set $\mathcal{D}_3$ consists of the five Dyck words

$$((())), \quad (()()), \quad (())(), \quad ()(()), \quad ()()().$$

Each word w determines a height profile $H_w(k)$ for $k = 0, \ldots, 6$, and an associated discrete area

$$A(w) = \sum_{k=0}^{5} H_w(k).$$

These quantities are listed in Table 1.

Dyck word w	height profile $H_w(k)$	$A(w)$
((()))	$(0, 1, 2, 3, 2, 1, 0)$	9
(()())	$(0, 1, 2, 1, 2, 1, 0)$	7
(())()	$(0, 1, 2, 1, 0, 1, 0)$	5
()(())	$(0, 1, 0, 1, 2, 1, 0)$	5
()()()	$(0, 1, 0, 1, 0, 1, 0)$	3

Table 1: Dyck words at semilength $n = 3$, with height profiles and discrete areas.

C.4 Coherent summation and interference

Assign to each history the complex weight

$$\psi(w) = e^{i\alpha A(w)},$$

as in Section 4. Let $x \in \mathcal{X}$ be a fixed observable outcome such that multiple histories from both source cones satisfy $f(w) = x$.

The amplitude associated with x is

$$\Psi(x) = \sum_{w:\, f(w)=x} e^{i\alpha A(w)}.$$

Because the observable discards source information, contributions from the left and right cones are summed coherently. Histories with equal area contribute the same phase, while histories with different distributions of height contribute distinct phases. Depending on the relative values of $A(w)$, the sum may exhibit constructive or destructive interference.

By contrast, a classical counting model would assign the weight

$$N(x) = \#\{w \in \mathcal{D}_n : f(w) = x\},$$

which cannot produce cancellation. The difference between $|\Psi(x)|^2$ and $N(x)$ is therefore entirely due to coherent summation over indistinguishable histories.

C.5 A worked finite example

Take $n = 4$ and choose two admissible Dyck prefixes of equal length and height,

$$u_L = \texttt{((}, \qquad u_R = \texttt{)(}(,$$

each of length 4 and height 2. Each prefix admits exactly three completions to a full Dyck word of length 8, yielding six histories in the union of the two source cones.

Define a coarse observable that discards source information by sampling the height at a fixed time step after the "slits":

$$f(w) := H_w(6) \in \{0, 2\}.$$

This is a discrete analogue of recording transverse displacement at a detector time without access to which slit was taken.

cone	w	$A(w)$	$f(w) = H_w(6)$
L	`((()(()))`	12	2
L	`((()()())`	10	2
L	`((())()()`	8	0
R	`)(((()))`	10	2
R	`)((()())`	8	2
R	`)((())()`	6	0

Table 2: Two equal-height source cones at $n = 4$ and a coarse detector observable.

With phase $\psi(w) = e^{i\alpha A(w)}$, the detector amplitudes are

$$\Psi(2) = \sum_{f(w)=2} e^{i\alpha A(w)} = e^{i12\alpha} + 2e^{i10\alpha} + e^{i8\alpha} = 2e^{i10\alpha}\big(1 + \cos(2\alpha)\big),$$

$$\Psi(0) = \sum_{f(w)=0} e^{i\alpha A(w)} = e^{i8\alpha} + e^{i6\alpha} = 2e^{i7\alpha}\cos(\alpha).$$

Classically one would predict multiplicities $N(2) = 4$ and $N(0) = 2$. In contrast, the quantum intensities $|\Psi(x)|^2$ vary with α and can exhibit strong suppression. For example, at $\alpha = \pi/2$ one obtains $\Psi(2) = 0$ (exact destructive interference at the outcome $x = 2$), even though $N(2) = 4$ histories contribute.

This example is intentionally tiny: its purpose is to show, in finite combinatorial terms, how (i) multiple histories per outcome, (ii) an additive phase functional, and (iii) coarse observation together produce interference. Larger n yields richer outcome sets and more intricate cancellation patterns.

C.6 Interpretation

No wave equation, spatial geometry, or continuum approximation has been assumed in this construction. Interference arises solely from three ingredients:

(i) multiple admissible histories,

(ii) an additive structural phase functional,

(iii) coarse-graining that renders distinct histories indistinguishable.

This mirrors the logical structure of the continuum double-slit experiment, but here the phenomenon is entirely discrete and combinatorial.

C.7 A pedagogical coarse-graining limit

For intuition, one may further coarse-grain the observable or rescale α so that phases reduce to $\psi(w) \in \{+1, -1\}$. In this limit, interference appears as signed counting over equivalence classes of histories. This toy limit is purely pedagogical and plays no role in the formal development of the theory.

C.8 Summary

This appendix demonstrates that the kinematic core of interference phenomena is already present on the Catalan light cone. Distinguishability is determined by the observable rather than by the ontology of histories, and coherent summation over indistinguishable combinatorial paths suffices to produce interference patterns familiar from continuum quantum mechanics.

D Computational Foundations

This appendix collects the formal background supporting the use of the Catalan substrate as a universal space of program structures and computational histories. The material here provides precise statements and examples for readers wishing to verify the correspondence between full binary trees, combinatory calculi, and rewrite dynamics.

Proof Sketch (of Proposition 3.1). As described in classical treatments of combinatory logic and the λ-calculus [8, 4], application is a binary operation, and every term therefore possesses a unique representation as a full binary tree: internal nodes encode application, and leaves encode variables, constants, or combinators. This establishes a canonical embedding of programs into $\mathcal{C}$.

Conversely, any full binary tree with labeled leaves may be interpreted as a well-formed program term by reading internal nodes as applications and leaves as atomic symbols, yielding a unique term up to α-equivalence.

Operational semantics are defined via local tree rewrites. A β-redex $(\lambda x.M)\,N$ contracts by replacing the parent application with $M[x := N]$; SKI reductions replace specific subtrees according to fixed patterns. In each case, the output remains a full binary tree, so evaluation never leaves $\mathcal{C}$. Because nondeterministic redex choices correspond to branching in the space of trees, each complete reduction sequence is a path through the Catalan possibility space, completing the correspondence. □

D.1 Binary Trees as Universal Program Frames

The identification of Catalan objects with program structures is a standard but essential foundation for the present work. Let $\mathcal{C}$ denote the set of full binary trees. A term in a functional calculus is constructed by repeated application, and an application $M\,N$ is represented by a binary node whose children encode M and N:

$$(M\,N) \quad \mapsto \quad \begin{array}{ccc} & \bullet & \\ M & & N \end{array}$$

This mapping is bijective between program terms (modulo α-conversion) and labeled elements of $\mathcal{C}$.

Pairs-expansions of combinators—for example the standard expansions of S and K into λ-terms—produce larger trees but remain within the Catalan family. Thus the Catalan substrate is closed under syntactic elaboration.

Operational semantics are likewise internal. Both β-reduction and SKI contraction replace subtrees with simpler subtrees while preserving the global full-binary-tree form. Each admissible reduction path therefore corresponds to a trajectory within $\mathcal{C}$, and nondeterminism in reduction strategy corresponds to branching structure within the Catalan tree itself.

This uniformity demonstrates that the Catalan substrate simultaneously captures:

1. program syntax (binary application structure),
2. program elaboration (via pairs-expansion or substitution), and
3. program dynamics (via evaluation rewrites).

Consequently, computation lives entirely within the Catalan family, justifying its use as the structural substrate for the unified causal–computational model developed in the main text.

D.2 Illustrative Figures

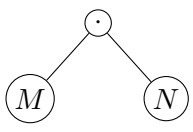

Figure 7: A binary application node representing the term $M\,N$.

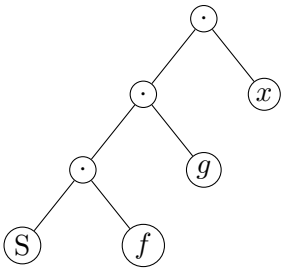

Figure 8: Binary-tree representation of the term S $f\,g\,x$.

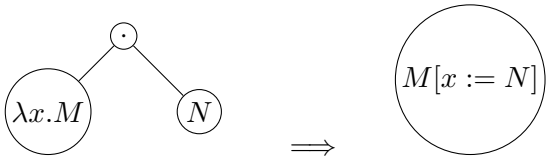

Figure 9: β-reduction as a local rewrite inside the Catalan family.

D.3 Pairs Expansion as Variable-Free S-Expressions

A central observation motivating this work is that the pairs expansions of combinators can be written as *variable- and label-free* S-expressions, exactly in the style of McCarthy's original Lisp notation [14]. In McCarthy's formulation, the core data structure is the cons-cell, written as a parenthesized pair. Here we push this idea to an extreme: we erase all atom labels and regard the program itself as a pure cons-tree, encoded only by balanced parentheses.

Concretely, consider the binary application tree for the term S $f\,g\,x$ (as in Figure 8). Under the pairs encoding used in our simulations, this same shape appears as the variable-free S-expression

```
((()(()(()()))))
```

.

This S-expression can also be understood as *looking down into* the underlying Catalan tree: the outer parentheses form the root frame, while each `()` corresponds to a leaf. The corresponding unlabeled binary tree shape is shown below.

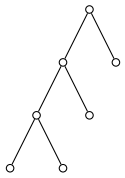

Viewed from this perspective, the S-expression is simply the linear "parenthesis trace" of this structure: each "(" corresponds to descending into a cons-cell, each ")" corresponds to returning toward the trunk, and the empty pairs `()` mark the terminal leaves.

More generally, the pairs bijection

```
n=0, c=1:  ()
n=1, c=1:  (()())
n=2, c=2:  (()(()())) ((()())())
n=3, c=5:  (()(()(()()))) (()((()())())) ((()())(()())) ((()(()())())()) ((((())())())())
```

enumerates exactly the same Catalan shapes that appear as Dyck paths

```
n=1, c=1:  ()
n=2, c=2:  (()) ()()
n=3, c=5:  ((())) (()()) (())() ()(()) ()()()
```

but seen through a different projection. The Dyck words present the one-dimensional "height" profile of the walk, making the Lorentzian scaling limit and the breadth–depth structure of the light cone transparent. The pairs S-expressions, by contrast, foreground the *binary computational structure*: they are precisely the unlabeled S-expression trees of a Lisp-like language, with cons as the sole constructor. [1]

In this sense, Dyck words and pairs expansions are two complementary Catalan bijections:

- Dyck words: a one-dimensional time–breadth profile well adapted to continuum limits and Lorentzian geometry;
- pairs S-expressions: a fully binary application tree well adapted to combinatory computation.

Both encode the same Catalan shapes; one may view them as distinct "Lorentz frames" on the same underlying combinatorial substrate. The pairs expansion can thus be regarded as an additional invariant transform: it preserves the Catalan class while re-expressing the same light-cone structure in purely computational coordinates.

There is also an intrinsic handedness in this picture. Dyck words of a given semilength n are not symmetric under reversal of the walk; the distribution of shapes across the tier reflects the left-to-right order in which parentheses are added. This asymmetry is the combinatorial trace of the fundamental handedness of applicative collapse in the pairs expansion: application is not commutative, and the collapse rule is oriented. The sequential construction of the S-expression tree makes this visible as a bias in how breadth is accumulated relative to depth.

A further simplification arises when we observe that in the S-expression view, explicit application nodes disappear entirely. Application is seen as a *property of the parentheses themselves*: a nested pair structure is already an applicative program. From the standpoint of Schönfinkel's combinatory logic [17], where even the familiar S and K can be reduced to a single sufficiently expressive combinator, one may heuristically say that if a lone combinator J acting on parentheses is enough, then we can omit J and work directly with the bare parentheses (). The Catalan substrate then becomes a *combinator-free* calculus of pure application.

Traditional functional calculi admit multiple evaluation strategies (normal-order, applicative-order, call-by-need, etc.). The Catalan substrate makes explicit a natural causal preorder on redex positions (ancestor order), constraining dependencies between contractions. Collapse is local, and contractions supported on disjoint subtrees commute (Lemma D.1). Different evaluation strategies may then be viewed as different linearizations of the residual freedom to schedule causally independent contractions (Appendix D).

Historical Perspective. The S-expression viewpoint connects the present framework to three classical constructions. First, McCarthy's original Lisp treats cons-pairs as the sole data constructor, with atoms added as a separate syntactic category [14]. Here we invert the hierarchy: structure is primary, and atoms—if present at all—arise as designated structural motifs.

[1] Here "projection" is not a literal mapping but a change of coordinates on the same Catalan object. The Dyck, binary-tree, and S-expression representations are all related by canonical bijections; each is a different parametrization of the same underlying Catalan shape. Thus switching from Dyck words to pairs S-expressions does not change the object itself, only the coordinate system through which it is viewed.

Second, Church encodings demonstrate that data and control structures can be represented entirely by higher-order functions; similarly, SKI combinatory logic eliminates variables altogether. These developments show that symbolic reference is not primitive but can be reconstructed from purely structural or operational primitives.

Third, Gödel numbering treats syntax as arithmetic structure. The present approach may be viewed as a "Catalan numbering," where syntactic entities are mapped to unlabeled binary trees. The Dyck, pairs, and binary-tree bijections then provide multiple coordinate systems for the same structural universe. In this sense, the Catalan substrate acts simultaneously as a computational calculus and as a structural semantics for symbolic systems.

D.4 Symbolic Representation in a Structure-Only Substrate

In the Catalan substrate all information is structural: the only primitive constructor is the cons-pair, and there are no atomic labels. This raises a fundamental question: how can a system without atoms support symbols, naming, or reference? The answer is that symbols arise not as primitives but as *structural motifs* that function as internal or external markers depending on context. We distinguish two forms of symbolic representation.

D.4.1 Internal Structural Symbols

Within a closed Catalan machine, one may bootstrap symbolic reference by designating particular tree shapes as internal "names." A higher-level self-referential mechanism (conceptually similar to a Y-like fixed-point operator) can maintain a dictionary of such shapes, mapping them to programs, behaviours, or combinator expansions. In this mode, names are themselves Catalan objects, and symbolic reference arises entirely from geometry: identifying a symbol is equivalent to matching a structural pattern. This yields a Lisp-like environment without atomic identifiers, where all "atoms" are implemented as canonical shapes in the tree.

D.4.2 External Structural Symbols

When interacting with external systems, the same structural motifs can serve as *extrinsic* symbols. Distinguished shapes may encode character codes, vector-drawing glyphs, device signals, or other forms of I/O. This does not modify the underlying calculus: it merely overlays a conventional interpretation on structural patterns. The Catalan substrate remains atomless internally, while external systems treat designated shapes as meaningful codes.

D.4.3 Unified View: Symbols as Distinguished Motifs

Both internal and external naming mechanisms exemplify a common principle: in a structure-only universe, symbols are not primitive entities but *designated Catalan motifs*. A symbol is simply a tree pattern endowed—internally or externally—with stable semantic interpretation. The substrate itself does not distinguish between data and code, or between program and identifier; all such distinctions emerge from the placement and recognition of specific structural forms.

Definition D.1 (Structural Symbol)**.** *A* structural symbol *is a finite Catalan tree S together with an interpretation map ι assigning S either (i) an internal computational meaning within the Catalan machine, or (ii) an external semantic meaning communicated to an outside system. The substrate recognizes S only as a structure; all semantics flow from ι.*

Remark D.1. *Although traditional programming languages begin with atoms and build structure on top of them, the Catalan substrate inverts this perspective: structure comes first, and atoms (if needed) are reintroduced later as structural patterns. From this viewpoint Lisp's cons-based representation, and even Schönfinkel's proposal of a single universal combinator, appear naturally as degenerate cases of a more general structure-first semantics.*

D.5 Causal Admissibility of Redex Contraction

We now formalize the sense in which evaluation order is fixed by causality rather than chosen by convention.

Definition D.2 (Causal Preorder on Positions)**.** *Let T be a full binary tree in the Catalan substrate, representing a program term. A* position *in T is a node address p in the usual tree sense (e.g. a finite word over $\{L, R\}$ indicating left/right choices from the root). We write $p \prec q$ if the node at position p lies on the unique path from the root to the node at position q. The reflexive, transitive closure of $\prec$ defines a preorder $\preceq$ on positions, which we call the* causal preorder*.*

Intuitively, $p \preceq q$ means that the subtree at q is causally downstream of the subtree at p: any change at p may propagate to q but not conversely.

Definition D.3 (Redex and Causal Admissibility)**.** *A* redex *in T is a position p such that the subtree rooted at p matches the left-hand side of a reduction rule (e.g. a β-redex or an SKI contraction). Let $R(T)$ be the set of all redex positions in T.*

A redex at position $p \in R(T)$ is causally admissible *if there is no other redex $q \in R(T)$ with $q \prec p$. In other words, a redex is causally admissible if it is minimal in $R(T)$ with respect to the strict causal order.*

Definition D.4 (Causally Admissible Reduction Sequence)**.** *A finite or infinite sequence of trees*

$$T_0 \to T_1 \to T_2 \to \cdots$$

is causally admissible *if, for each step $T_i \to T_{i+1}$, the contracted redex is causally admissible in T_i in the above sense. A* causal computation *is a causally admissible sequence starting from some initial tree T_0.*

Lemma D.1 (Commutation of disjoint reductions)**.** *Let T be a Catalan tree (full binary tree) and let $p, q \in R(T)$ be two redex positions that are* incomparable *under the causal preorder $\preceq$ (i.e. neither lies on the path from the root to the other). Let T_p denote the result of contracting the redex at p, and similarly T_q. Then q remains a redex position in T_p and p remains a redex position in T_q, and contracting both redexes yields the same tree regardless of order:*

$$(T_p)_q \;\equiv\; (T_q)_p.$$

In particular, disjoint reductions form a commuting diamond as in Figure 6.

Proof Sketch. Since p and q lie in disjoint subtrees, contracting at p rewrites only the subtree rooted at p and leaves the subtree rooted at q unchanged. Thus the redex at q is unaffected (and remains at the same position), so it may still be contracted in T_p. Symmetrically, contracting at q leaves the subtree at p unchanged. Because the two rewrite steps act on disjoint parts of the tree, performing both contractions yields the same result regardless of order. □

D.6 Evaluation Strategies as Coarse-Grainings of Causal Order

Traditional presentations of the λ-calculus distinguish several evaluation strategies: normal-order, applicative-order, call-by-need, and many others. These are usually defined syntactically (e.g. by specifying which redex is chosen at each step), with confluence guaranteeing that they terminate in the same normal form when one exists. In the Catalan substrate, however, causality constrains redex selection more tightly.

Definition D.5 (Strategy-Compatible Causal Computation)**.** *Let $\mathcal{S}$ be a syntactic evaluation strategy (e.g. normal-order or applicative-order) which, given a term, selects one or more redex positions considered "eligible" at each step. A causal computation*

$$T_0 \to T_1 \to \cdots$$

is compatible *with $\mathcal{S}$ if, at each step, the contracted redex is both causally admissible in T_i and belongs to the set of redexes selected by $\mathcal{S}$ for the corresponding term.*

Proposition D.1 (Strategies as Coarse-Grainings of Causal Structure)**.** *Let T_0 be an initial term, and suppose $\mathcal{S}$ is a standard evaluation strategy that is normalizing on T_0 (e.g. normal-order for a weakly normalizing term). Then:*

1. *Every $\mathcal{S}$-guided reduction sequence can be refined to a causally admissible computation by reordering only reductions that occur at redexes incomparable under the causal preorder.*
2. *Conversely, every causally admissible computation from T_0 to normal form projects to an $\mathcal{S}$-valid history by forgetting the precise interleaving of causally independent reductions.*

In this sense, classical evaluation strategies are coarse-grainings of the underlying causal order: they differ only in how they resolve the residual freedom to permute causally independent redex contractions.

Proof Sketch. For (1), observe that any $\mathcal{S}$-guided sequence that temporarily contracts a non-minimal redex (with respect to $\preceq$) must do so in a context where all redexes on which it causally depends will eventually be contracted as well. By standard commuting-conversion arguments, we can reorder the sequence so that causally prior redexes are contracted first, without changing the final normal form. This reordering affects only redexes that lie in disjoint subtrees, i.e. are incomparable under $\preceq$.

For (2), given a causally admissible computation, we can group together all contractions that $\mathcal{S}$ regards as taking place at the "same" redex position in the syntactic term, ignoring the precise ordering among contractions in disjoint subtrees. The resulting abstract history matches what $\mathcal{S}$ would produce, by confluence and the fact that $\mathcal{S}$ is normalizing on T_0. Thus $\mathcal{S}$ may be seen as a projection that forgets the fine-grained causal structure of independent collapses while preserving the global reduction behaviour. □

References

[1] L. Addario-Berry, L. Devroye, and S. Janson. Sub-Gaussian tail bounds for the width and height of conditioned Galton–Watson trees. *Annals of Probability*, 41(2):1074–1087, 2013.

[2] J. Ambjørn, J. Jurkiewicz, and R. Loll. Dynamically triangulating Lorentzian quantum gravity. *Nuclear Physics B*, 610:347–382, 2001.

[3] J. Ambjørn, A. Görlich, J. Jurkiewicz, and R. Loll. Nonperturbative quantum gravity. *Physics Reports*, 519:127–210, 2012.

[4] H. P. Barendregt. *The Lambda Calculus: Its Syntax and Semantics*. North-Holland, 1984.

[5] L. Bombelli, J. Lee, D. Meyer, and R. D. Sorkin. Space-time as a causal set. *Physical Review Letters*, 59(5):521–524, 1987.

[6] A. Church. A set of postulates for the foundation of logic. *Annals of Mathematics*, 34:839–864, 1933.

[7] T. M. Cover and J. A. Thomas. *Elements of Information Theory*. 2nd edition, John Wiley & Sons, 2006.

[8] H. B. Curry and R. Feys. *Combinatory Logic, Vol. I*. North-Holland, 1958.

[9] H. B. Curry. *Foundations of Mathematical Logic*. McGraw–Hill, 1958.

[10] R. P. Feynman and A. R. Hibbs. *Quantum Mechanics and Path Integrals*. McGraw–Hill, 1965. (Dover reprint, 2010).

[11] S. Janson. Brownian excursion area, Wright's constants in graph enumeration, and other Brownian areas. *Probability Surveys*, 4:80–145, 2007.

[12] M. Kac. On distributions of certain Wiener functionals. *Transactions of the American Mathematical Society*, 65(1):1–13, 1949.

[13] J.-F. Le Gall. Random trees and applications. *Probability Surveys*, 2:245–311, 2005.

[14] J. McCarthy. Recursive functions of symbolic expressions and their computation by machine, Part I. *Communications of the ACM*, 3(4):184–195, 1960.

[15] R. Orús. A practical introduction to tensor networks: Matrix product states and projected entangled pair states. *Annals of Physics*, 349:117–158, 2014.

[16] C. Rovelli. *Quantum Gravity*. Cambridge University Press, 2004.

[17] M. Schönfinkel. Über die Bausteine der mathematischen Logik. *Mathematische Annalen*, 92:305–316, 1924.

[18] R. P. Stanley. *Catalan Numbers*. Cambridge University Press, 2015.